

BEHAVIOR OF HIGH STRENGTH CONCRETE R.C. BEAMS MIXED WITH DISCRETE GLASS FIBER

¹Dr. Moustafa Osman, ²Dr. Magdy M, ³AYMAN.A. EL-ASHHAB.

¹Associate Professor of Civil Engineering, Faculty of Engineering, Helwan University

²Assistant Professor of Civil Engineering, Faculty of Engineering, Helwan University

³Master of Science Graduate of Civil Engineering, Faculty of Engineering, Helwan University

Abstract: During the last four decades, glass fiber reinforced concrete has increasingly been used in structural applications. It is generally accepted that the addition of glass fibers significantly increases tensile toughness and ductility, also slightly enhances the compressive strength. Several studies have reported previously the favorable attributes of glass fiber reinforced concrete (GFRC) on compression, tension and shear behavior. As the models proposed so far can, at best, describe only a few aspect of the GFRC with a given type and amount of fibers, establishing simple and accurate, generalized equations to describe the behavior of the GFRC in tension, compression and shear that take into account the fiber type and content is essential. This research investigated the shear behavior of GFRC and to formulate a generalized model for the ultimate shear strength of GFRC. Effect of the fiber volume fraction on the shear response of GFRC with optimum glass fiber content has been studied. Four different volume contents ranging from 0% to 1.5% was used in the test specimens. Direct shear tests were conducted and finally, an equation model was proposed to predict the ultimate shear strength of GFRC in terms of glass fiber content.

Keywords: glass fiber; discrete GFRC, high strength concrete.

1. INTRODUCTION

Glass fiber reinforced concrete (GFRC) is a cement based composite product that is reinforced with glass fibers. GFRC is a relatively new type of building material and increasingly being used in different countries and has many architectural applications. Adding of glass fibers to concrete mixes increase its durability and sturdiness. While the regular concrete mixes are normally used at a fraction of the weight, GFRC can be used any where. Among the main advantages of GFRC are lightweight, high moisture resistance, high compressive strength, low maintenance, low thermal expansion and high fire resistance respectively.

The problem of determining the shear strength of reinforced concrete beams not closed up to know. Thus, the shear strengths predicted by different current design codes for a particular R.C beam section can vary by a factor of greater than. In contrast, the flexural strengths predicted by the same codes are unlikely to vary by more than 10%. For the flexure behavior of R.C. beams, the plane sections hypothesis forms the basis of a universally accepted, simple, rational theory for predicting flexural strength. In addition, simple experiments can be performed on reinforced concrete beams subjected to pure flexure and the clear results from such tests have been used to improve the theory. In shear, there is no agreement for a rational theory and experiments can not be conducted on R.C. beams subjected to pure shear.

While hundreds of tests have been undertaken on the shear behavior of R.C. beams, the test pool of fiber-reinforced specimens are few. Fewer still are tests with fiber reinforced concrete members where the fiber concrete is designed to carry the full shear capacity.

The theory of concrete plasticity provides a good basis for the shear design of GFR-UHPC (Glass Fiber Reinforced-Ultra High-Performance Concrete) beams as the use of high quantities of ductile steel fibers in the concrete matrix leads to a relatively plastic response after cracking of the matrix with high tensile strengths maintained for large crack openings.

Previous results show that the nominal stress in shear cracking and the ultimate shear strength increased with the increasing fiber volume, decreasing shear span-to-depth ratio, and also increasing the concrete compressive strength. Moreover, as the fiber content increases, the failure changes from shear to flexure mode.

The diagonal shear failure of reinforced concrete beams has long been known to be a brittle type of failure. Therefore, a larger safety margin is provided by the capacity reduction factor in the codes. The present code formulas have been calibrated to provide adequate safety against the initiation of diagonal shear cracks. However, the crack initiation load is not proportional to the ultimate load. It can be much smaller, or only slightly, depending on the beam size and other factors. Therefore, the existing design formulas cannot be expected to provide a uniform safety margin against failure. Ideally, the design should insure proper safety margins against failure and crack initiation.

The primary purpose of inclusion of steel fibers in conventionally R.C. members is not for increasing strength. The strength can be increased more easily and economically by using steel bars placed along the direction of principal tensile stresses. The deficiencies of ordinary R.C. in the form of micro cracks, which can not be corrected by bar reinforcement, can be remedied to a significant extent by using fiber reinforcement. Addition of randomly oriented fibers in plain concrete mixes helps to bridge and arrest the cracks formed in the brittle concrete under applied stresses, and enhances the ductility and energy absorption properties of the composite.

The main objective of this search is to study the performance and the efficiency of using discrete glass fibers on the shear behavior of R.C. beams. Moreover, a comparison between the shear efficiency of increasing traditional transverse by using discrete glass fibers with stirrups is presented. Finally, the test failure loads are compared with the prediction shear values of the codes.

2. EXPERIMENTAL WORK

Twelve R.C. beams with a rectangular cross-section sized 120 mm (width) 250mm (height) 1500mm length, was manufactured and tested as shown in Fig. 1(a). Two parameters were considered in this study; variable discrete glass fiber ratio by weight, and shear span to Depth ratio. Details of these two parameters are shown in Table 1. The target concrete compressive strength is obtained from the average of three tested cubes (150 x 150 x 150 mm) from each batch.

Loads were applied by using a hydraulic jack of 550 KN capacity connected to a steel space frame. The four-point symmetrical loading with distance 150 mm between the loading points were statically applied to all tested specimens. All specimens were tested up to failure under incremental loading procedure.

Concrete mix used to cast the tested R.C. beams consisted of Portland cement, natural sand and gravel as aggregates and water. The mixing proportion of different materials was by weight of cement and the average characteristic concrete compressive strength for tested beams without fibers is 53 MPa and for beams with fiber ratios, 0.25% is 55Mpa, 0.75%, and 1.5% is 58MPa and 51MPa, respectively.

The properties of the used glass fibers are as follows: fiber length is 15 mm with Young's modulus of 72 GPa, a shear modulus of 29.1 GPa, an ultimate tensile strength of 1600 MPa, and an ultimate tensile strain of 2.2%, respectively (based on the manufacturer). Digital Load capacity of 550 kN with an accuracy of 0.1 kN was adopted to measure the applied loads. The values of the applied loads were recorded from the monitor connected to the load cell. The beams were tested using an incremental loading procedure. The vertical displacement of the tested beams was recorded using two electric dial gauges, one in the middle of the beams and the other at a distance equal to half of the beam depth from the support. The strains at the mid-span section were measured by using demec points. Fig. 1 shows the positions of the electrical strain gauges, dial gauges, and demec points. During tests, the applied load was kept constant at each load stage for measuring and observing.

3. TEST RESULTS AND ANALYSIS

In each beam was loaded the same span to depth ratio, the first flexural cracks (in the central zone) and shear cracks (in the shear spans) all specimens were also the same until the first diagonal shear cracking occurred.

The RC beams with glass fiber ratio, all failed in shear. The failure load in most cases was only slightly higher (more than 5%) than the first shear cracking load and some cases where finding the deflection values as it happened in the beam have remained fairly constant.

A reduction in the failure load of about 40% was noted for the beams loaded in 2.2 when compared to the ones loaded in 1.8 and 2.0, showing a tendency for the ultimate shear failure load to decrease with the increase.

The use of discrete glass fibers had a significant effect on the failure load with a shear span-to-depth ratio equal 1.80 shear span-to-depth ratio equal 2.0, respectively.

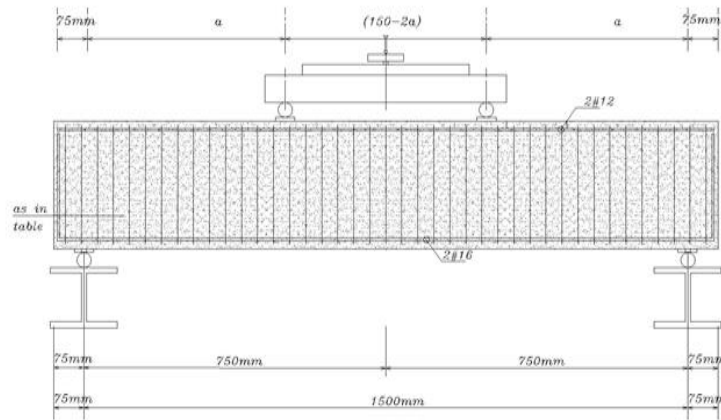


Figure 1(a): Details of test specimens

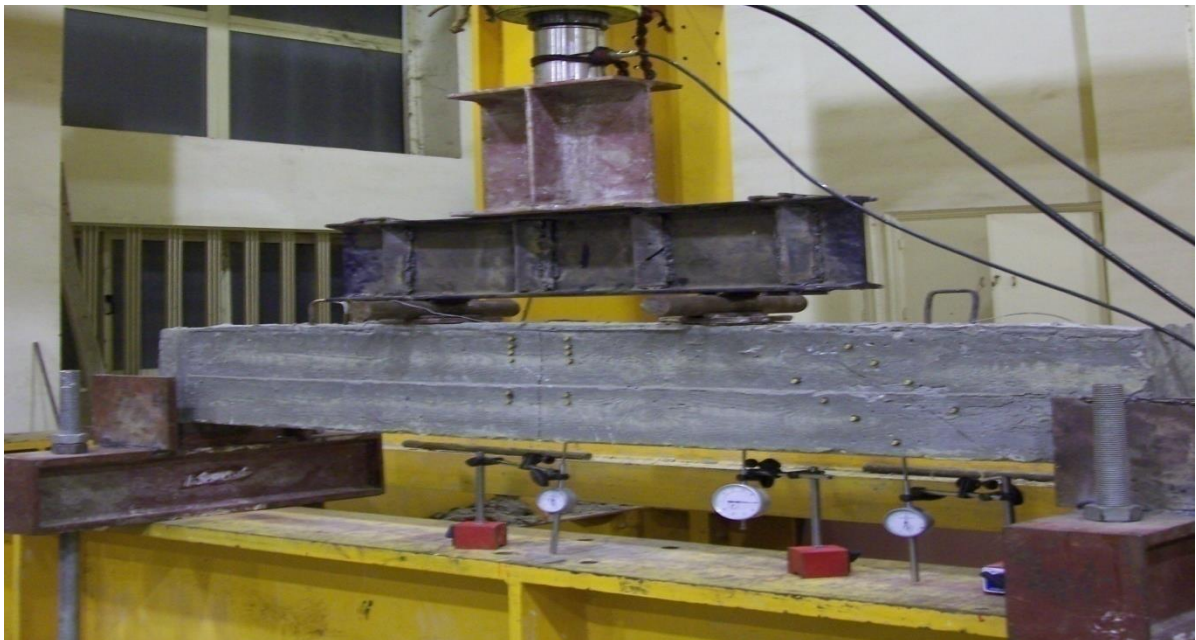


Figure 1(b): Test set-up and instrumentation

Table 1: Summary of studied parameters.

Group	dimension	specimens	Fiber content	a/d
Group No.1	120x250	S1	0%	1.8
	120x250	S2	0.25%	1.8
	120x250	S3	0.75%	1.8
	120x250	S4	1.50%	1.8
Group No.2	120x250	S5	0%	2
	120x250	S6	0.25%	2
	120x250	S7	0.75%	2
	120x250	S8	1.50%	2
Group No.3	120x250	S9	0%	2.2
	120x250	S10	0.25%	2.2
	120x250	S11	0.75%	2.2
	120x250	S12	1.50%	2.2

3.1 Crack pattern and mode of failure:

Crack patterns and failure modes for all tested beams are shown in Figures 2,3,4,5,6,7,8 ,9,10,11,12,13. The failure load and failure mode are presented in Table 2. The failure of tested beams without glass fiber showed a brittle failure mode compared to specimens with glass fibers. In the shear span, one or two major cracks together with some secondary cracks formed. The major crack propagated from the support to the point of loading as the load increased up to the beams failure. The crack patterns of the beams with mixed glass fiber were characterized closer and thinner cracks than that of beams without glass fiber. Finally, it is found that the spread area of external crack increased by increasing the percentage of discrete fiber from 0.25% to 0.75%.

The crack pattern describes the progress of cracks with loading up to failure. Generally, fine cracks started in the diagonal directions to a degree of 45°. For most tested specimens, the mode of failure was sheared. Table 2. Presents the type of failure for each tested beam. For specimens with a lower tension steel ratio (0.51%), flexural failure took place, while the mode of failure was combined flexure and shear failure (shear failure with ductility).

Table 2: Failure loads of tested specimens.

Group	dimension	specimens	Failure Load	Mode of Failure
Group No.1	120x250	S1	220	Flexural Shear
	120x250	S2	250	Compression Flexural
	120x250	S3	300	Diagonal Flexural
	120x250	S4	210	Diagonal Flexural
Group No.2	120x250	S5	250	Compression Flexural
	120x250	S6	270	Compression Flexural
	120x250	S7	270.5	Flexural
	120x250	S8	190	Shear
Group No.3	120x250	S9	200	Diagonal tension
	120x250	S10	180	Compression
	120x250	S11	110	Flexural
	120x250	S12	120	Web Shear Crushing

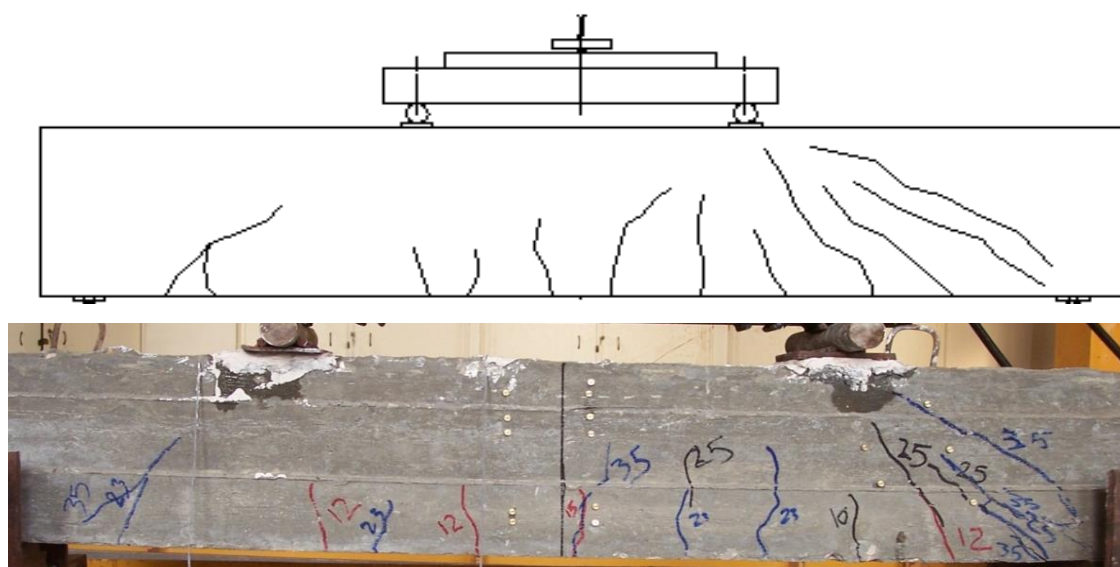


Figure (2): Crack patterns for specimen (S1) (zero fiber with Shear span-to-depth ratio 1.8).

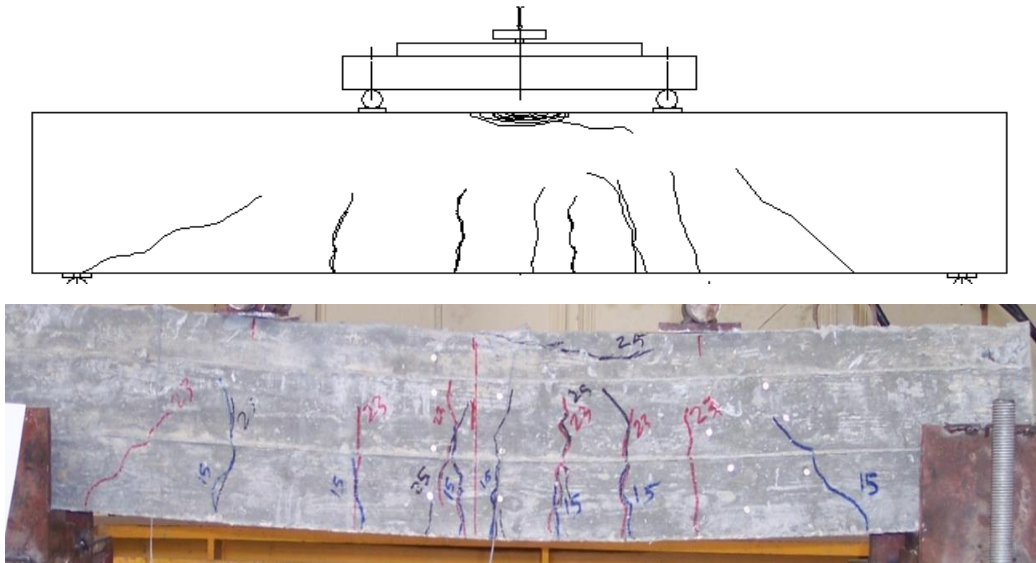


Figure (3): Crack patterns for specimen (S2) (0.25%fiber with Shear span-to-depth ratio 1.8)

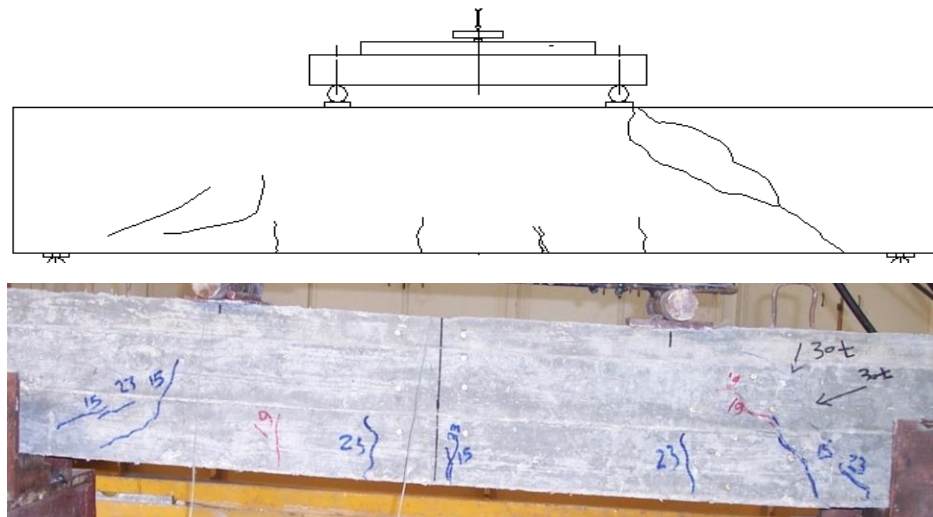


Figure (4): Crack patterns for specimen (S3) (0.75%fiber with Shear span-to-depth ratio 1.8)

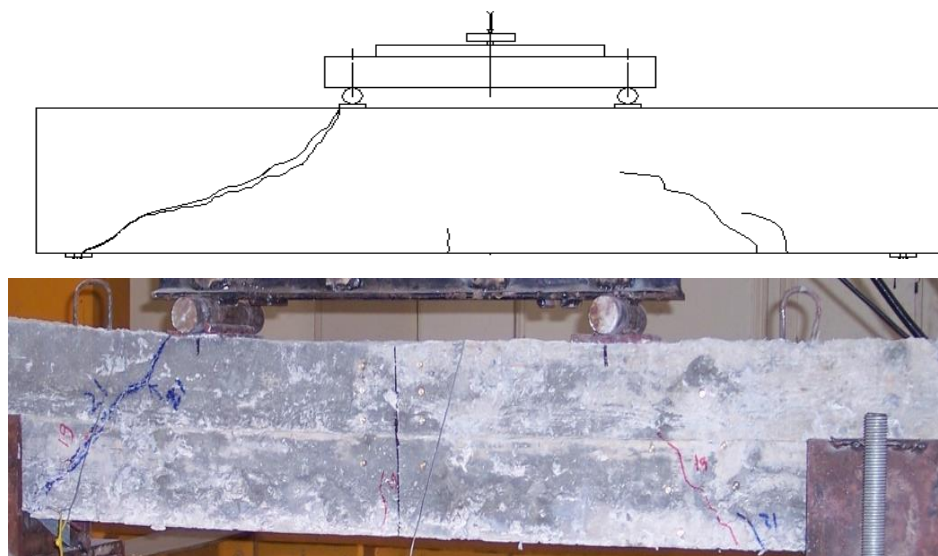


Figure (5): Crack patterns for specimen (S4) (1.5%fiber with Shear span-to-depth ratio 1.8)

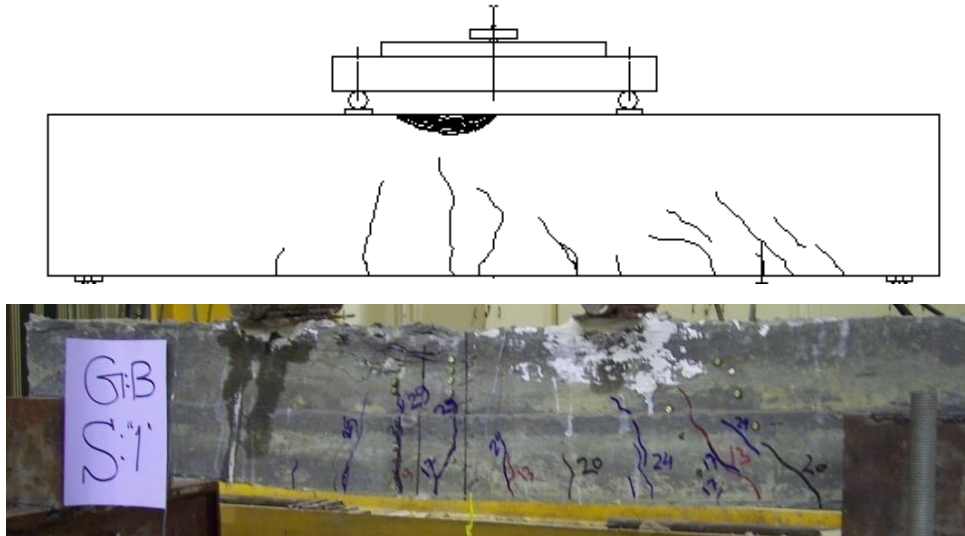


Figure (6): Crack patterns for specimen (S5) (0% fiber with Shear span-to-depth ratio 2)

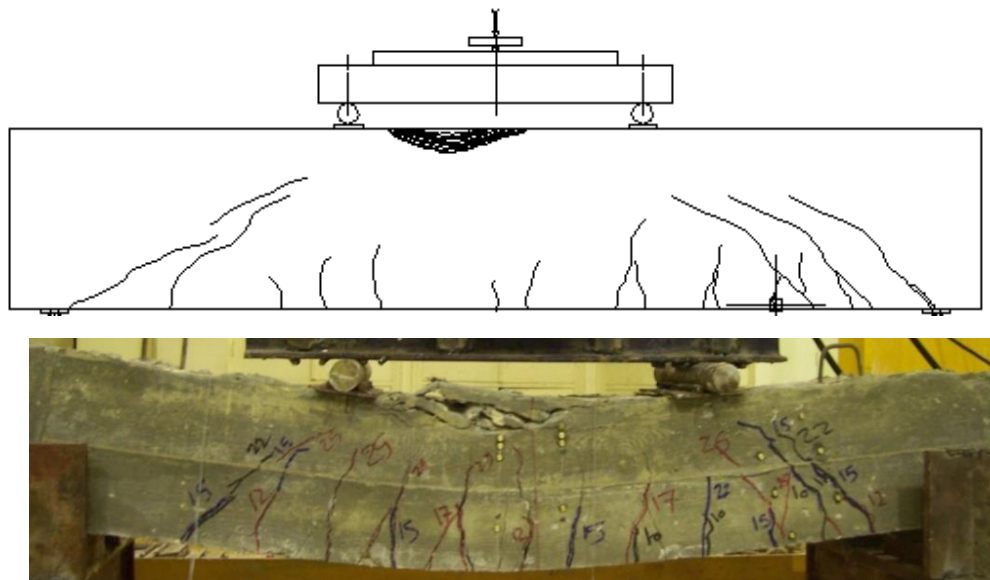


Figure (7): Crack patterns for specimen (S6) (0.25% fiber with Shear span-to-depth ratio 2)

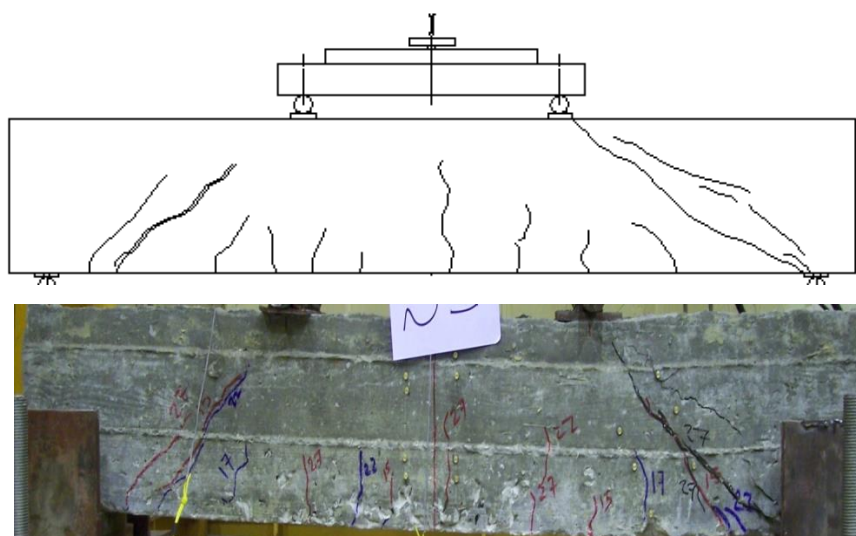


Figure (8): Crack patterns for specimen (S7) (0.75% fiber with Shear span-to-depth ratio 2)

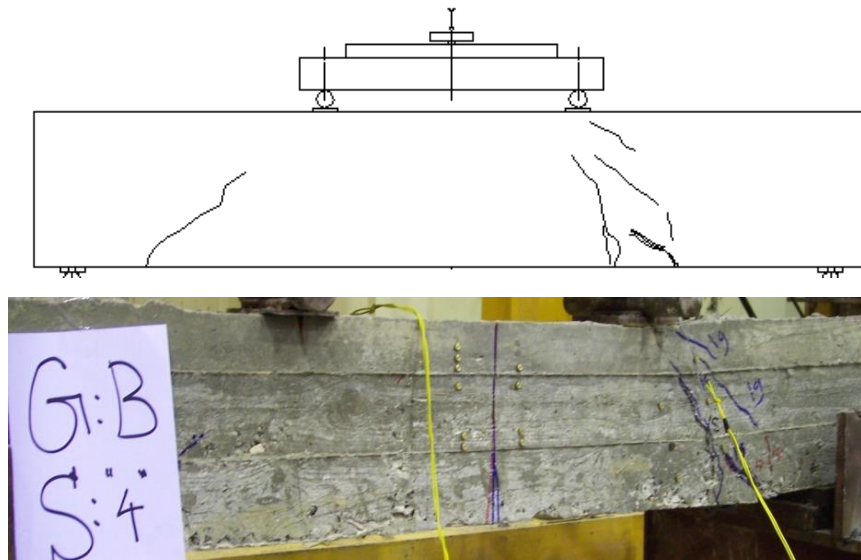


Figure (9): Crack patterns for specimen (S8) (1.5%fiber with Shear span-to-depth ratio 2)

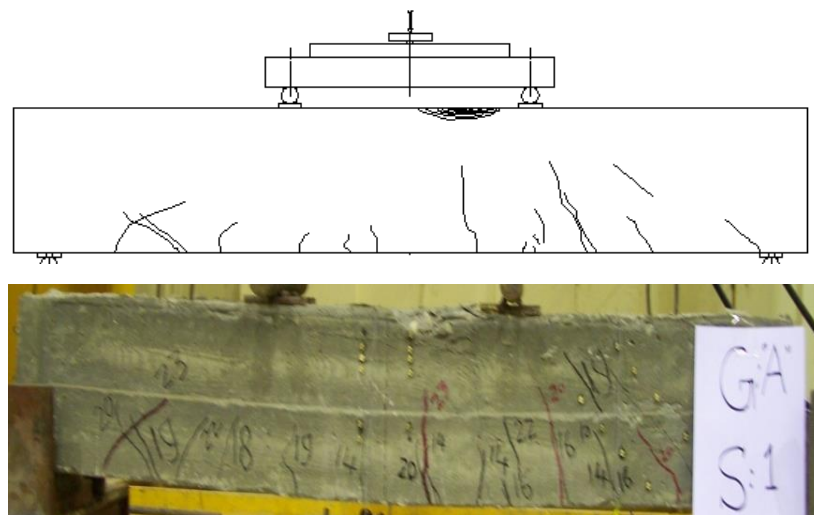


Figure (10): Crack patterns for specimen (S9) (0%fiber with Shear span-to-depth ratio 2.2)

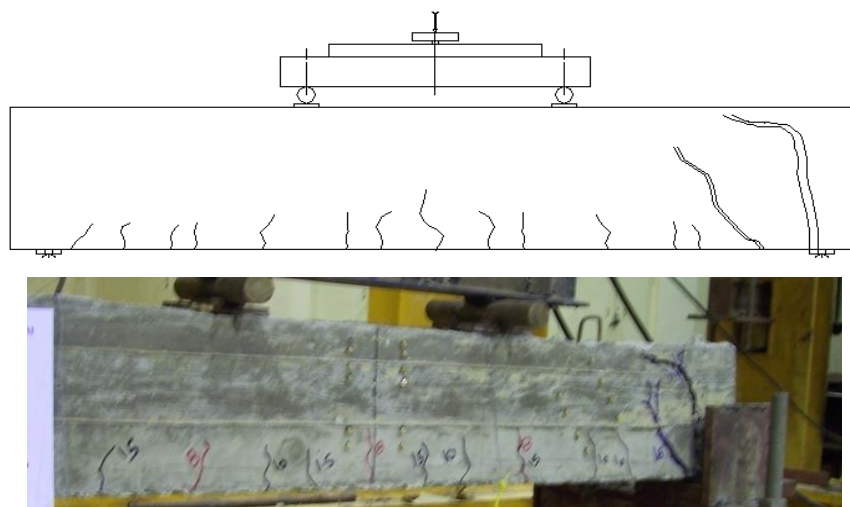


Figure (11): Crack patterns for specimen (S10) (0.25%fiber with Shear span-to-depth ratio 2.2)

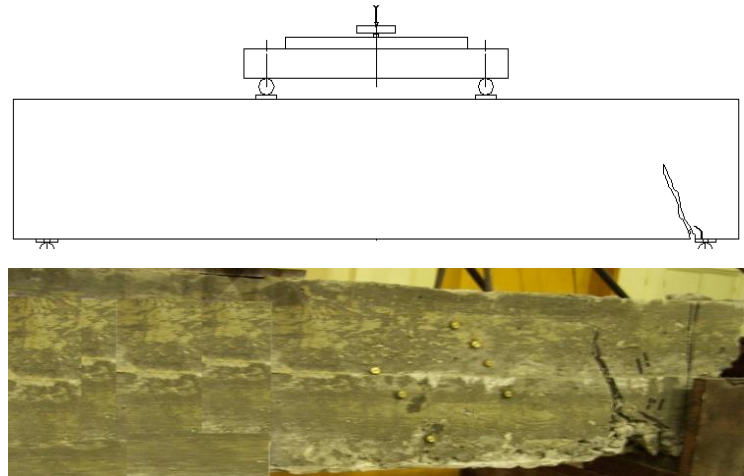


Figure (12): Crack patterns for specimen (S11) (0.75%fiber with Shear span-to-depth ratio 2.2)

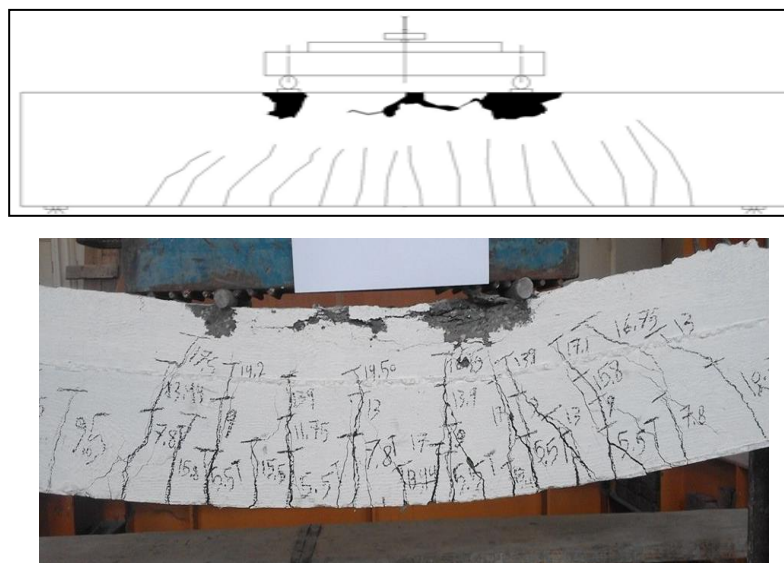


Figure (13): Crack patterns for specimen (S12) (1.5%fiber with Shear span-to-depth ratio 2.2)

3.2. Load Deflection Curves:

Figures. 14,15,16,17,18,19,20,21,22,23,24,25. shows the electrical strain distributions in two positions; the first at mid-span measures the strain in the tension reinforcement (2 Y16) and the second at a distance from the half depth of support fixed in the middle height of stirrups.

On the other hand, strain increasing rate at mid-span for tested glass fiber concrete beams is almost constant. By comparing the strain distributions of the beams with and without glass fiber, it is noticed that beams with glass fiber behave as a homogeneous material as the strain in tension nearly equal to that at compression zones.

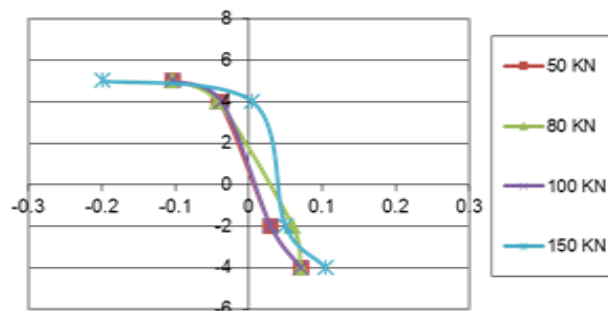


Figure (14): The strain distribution for tested beam S1 at the mid-span

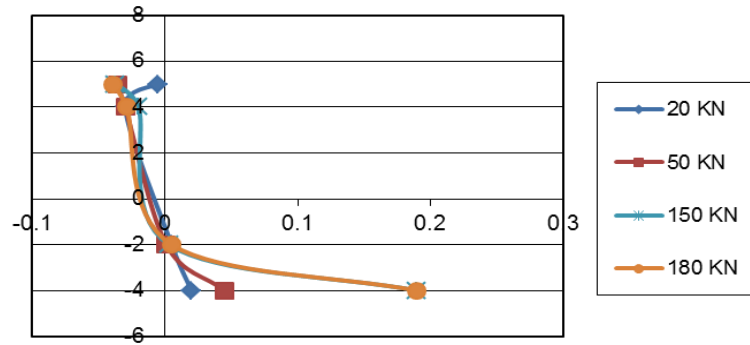


Figure (15): The strain distribution for tested beam S2 at the mid-span

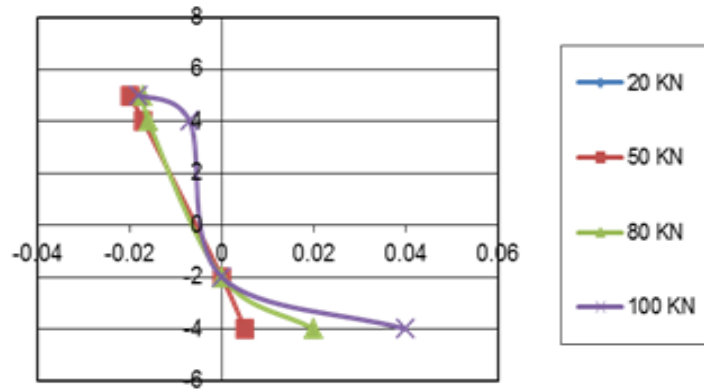


Figure (16): The strain distribution for tested beam S3 at the mid-span

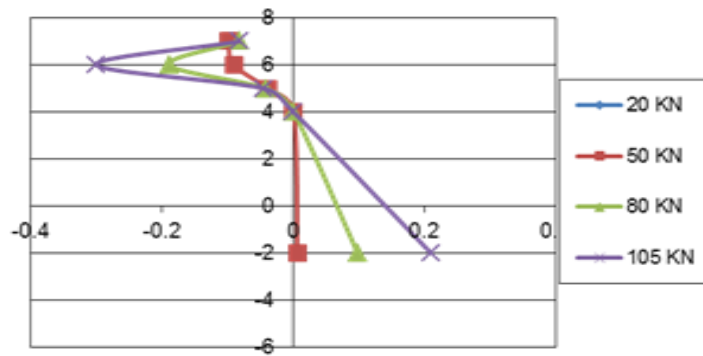


Figure (17): The strain distribution for tested beam S4 at the mid-span

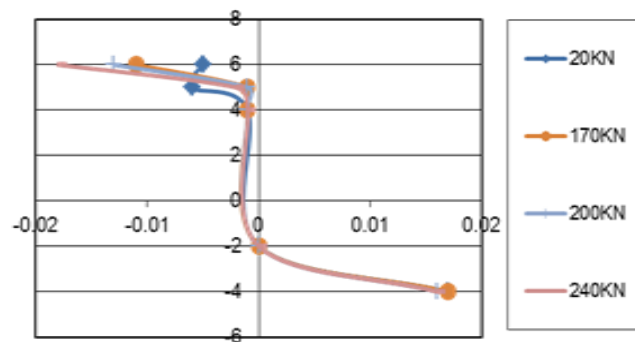


Figure (18): The strain distribution for tested beam S5 at the mid-span

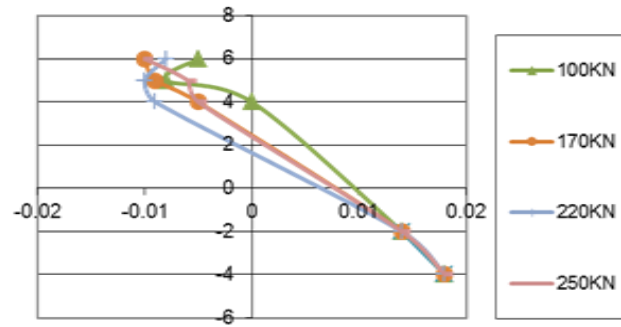


Figure (19): The strain distribution for tested beam S6 at the mid-span

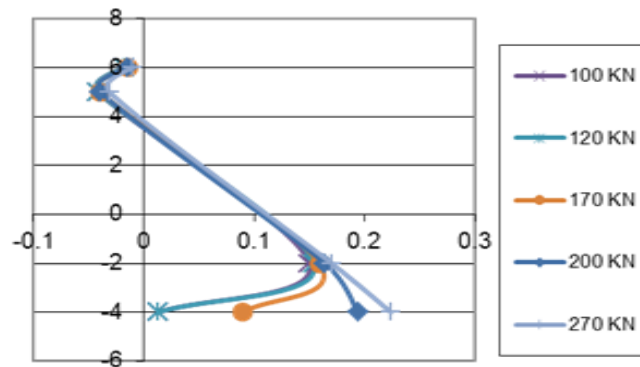


Figure (20): The strain distribution for tested beam S7 at the mid-span

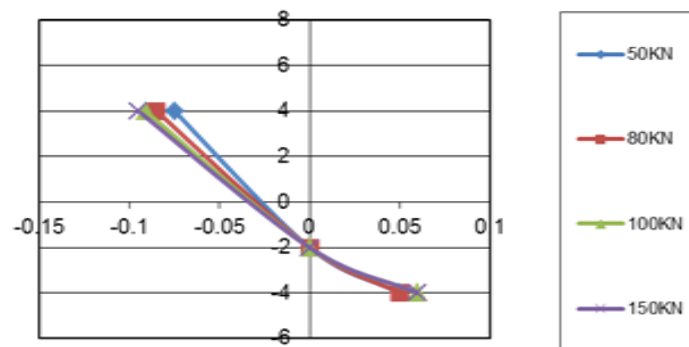


Figure (21): The strain distribution for tested beam S8 at the mid-span

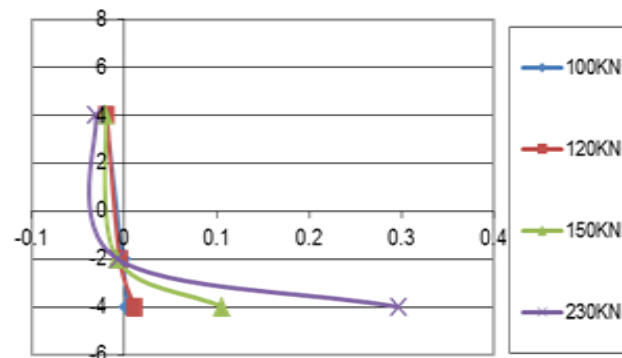


Figure (22): The strain distribution for tested beam S9 at the mid-span

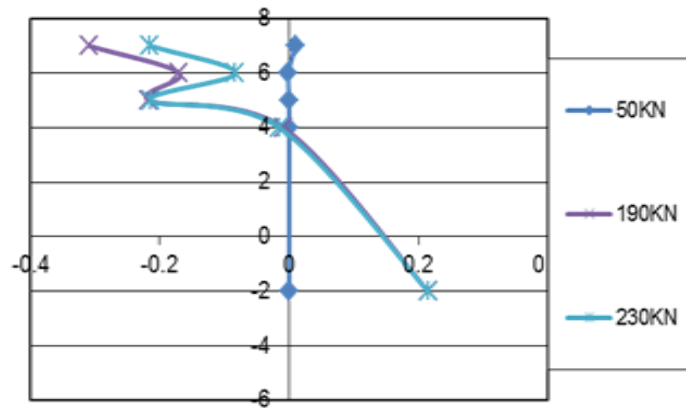


Figure (23): The strain distribution for tested beam S10 at the mid-span

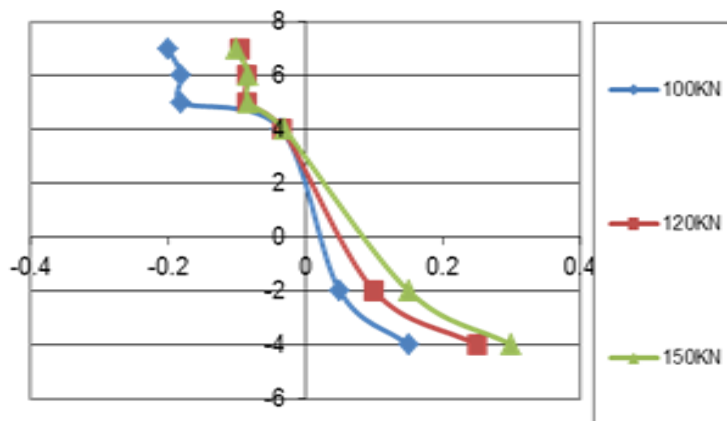


Figure (24): The strain distribution for tested beam S11 at the mid-span

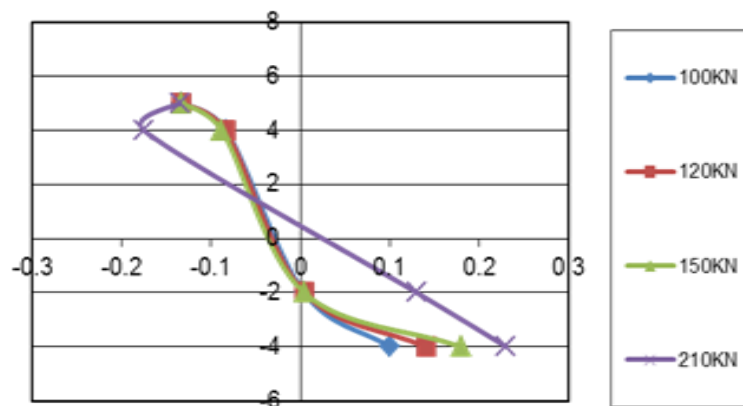


Figure (25): The strain distribution for tested beam S12 at the mid-span

3.3. Load Deflection relationship:

Figures 26,27,28,29 shows the relationship between the applied load and mid-span deflection for different shear span and depth ratio and different glass fiber ratios respectively. The increased ratio of glass fiber enhanced the stiffness of tested beams where decreasing the shear span and depth ratio nearly has an effect on the stiffness. Moreover, it is clear that the increase in the glass fiber ratio increases the maximum deflection and in turn increasing the shear ductility of the tested R.C. beams. On the other side, increasing the shear span and depth ratio leads to reducing the maximum deflection of the tested R.C. beams and a brittle failure is obtained.

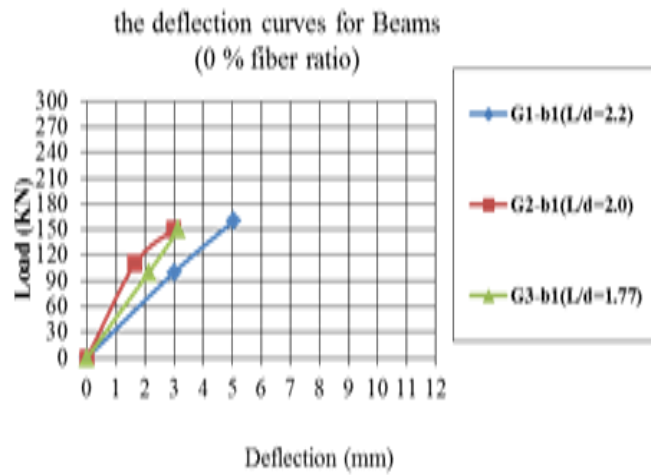


Figure (26): Load–deflection curves for tested specimens with zero % fiber ratio.

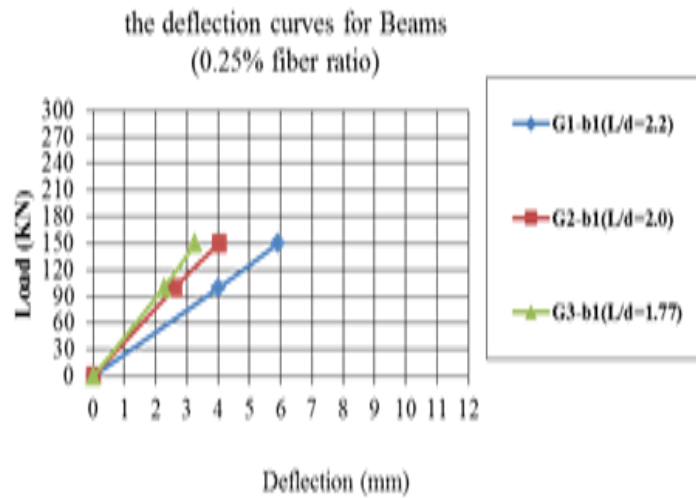


Figure (27): Load–deflection curves for tested specimens with 0.25 % fiber ratio.

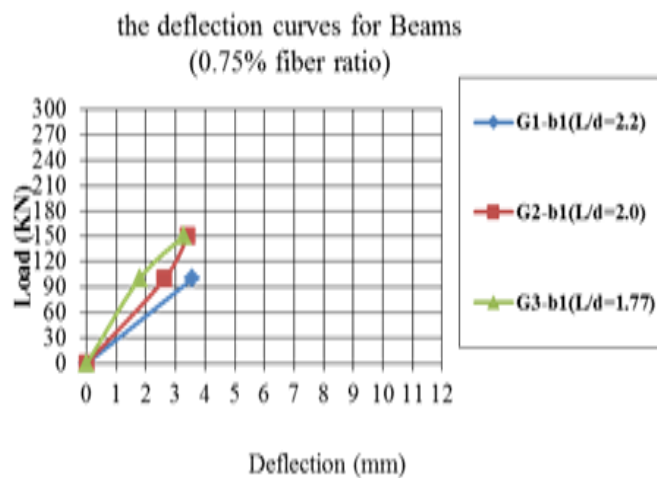


Figure (28): Load–deflection curves for tested specimens with 0.75 % fiber ratio.

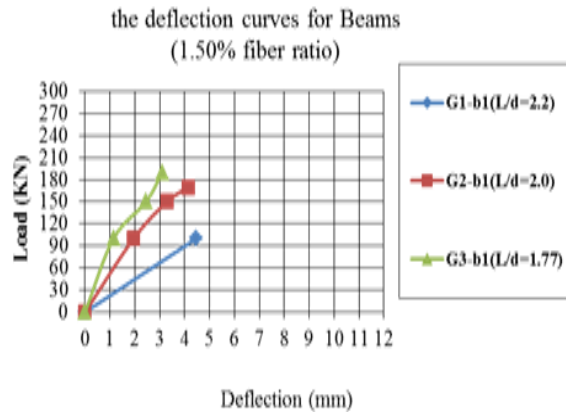


Figure (29): Load–deflection curves for tested specimens with 1.5 % fiber ratio.

4. THE EFFECT OF SHEAR SPAN TO DEPTH RATIO

In specimens with $a/d=1.8$ and 2.0 , diagonal shear cracks were observed at loads ranging from 37 % to 67% of the ultimate loads. In specimens with $a/d=2.2$, these cracks occurred at a stage close to failure. All test beams developed diagonal shear cracks and behaved essentially as tied arches until collapse. These cracks initiated along a line joining the loading and support points. Comparing the load-deflection of the test beams with the same amount of GFRC shows the significant increase effect of the ductility of the beams. Beams with $a/d=2.2$ exhibit brittle behavior, while it appears that beams with $a/d=1.8$ and 2.0 provide some warning of impending collapse. For beams with $a/d=2.2$, the failure was sudden.

It is generally recognized that increasing a/d decreases the shear strength for the same applied load

5. COMPARISON BETWEEN FAILURE LOADS FOR THE SPAN TO DEPTH RATIO

By comparing the test results in this study and test results with the same material properties and test setup. The relation between the failure load and fiber content with different span to depth ratio Fig 30, in general, by change ratio of L/d from 2.2 to 1.8 the failure load increased about 1.5 times. Moreover, by using discrete glass fiber with ratio 0.25%, 0.75% and 1.5% the load increased by about 1.4, 2.7 and 1.75, respectively.

From this, it is concluded that by increasing the span to depth ratio, the efficiency of discrete fiber is reduced. In addition, from this, it is concluded that the efficiency of using discrete glass fiber on the failure loads can be considered as efficient as that of vertical steel.

However, by comparing the crack patterns and modes of failure, it is found that the behavior is better when discrete glass fiber was used than when vertical stirrups were used. Where in the span to depth ratio 2.2 the failure mode changed from shear failure to flexure shear failure. And the number of cracks in specimens of the span to depth ratio 1.8 is increased at the bottom of beams near to support. The cracking load is decreased by increasing failure load.

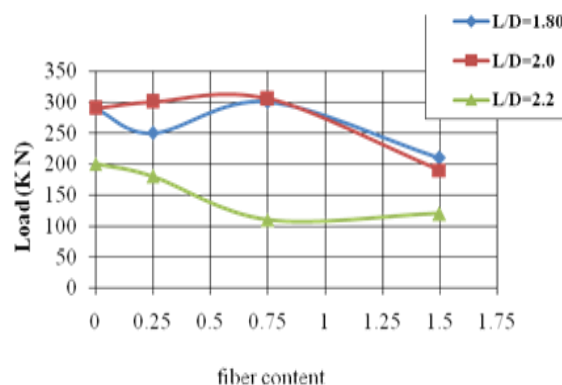


Figure 30: Comparing between failure loads for span to depth ratio

By comparing the strength for the span to depth ratio of 1.8 and 2.2, it was found that the shear strength in L/D=1.8 is more than that in L/D=2.2.

From studying the effect of the span to depth ratio on the shear failure and using discrete glass fiber, it was found that, by decreasing the span to depth ratio the efficiency of the used discrete glass fiber increased.

6. EVALUATION ACCORDING TO EGYPTIAN CODE (ECP-203) AND (ACI- CODE) (SHEAR AND FLEXURAL STRENGTH)

6.1 Proposed shear strength approach HSFRC beams:

Shear force is present in beams at sections where there is a change in bending moment along the span. An exact analysis of shear strength in a reinforced concrete beam is quite complex. Several experimental studies have been conducted to understand the various modes of failure that could occur due to a possible combination of shear and bending moment. Despite the great research efforts, the process is still not simple. In addition, many of the factors that influence the determination of the required minimum amount of shear reinforcement are not yet known. The shear strength of R.C. beams depends on the strength of concrete, the percentage of the longitudinal reinforcement and the span-to-depth ratio or stiffness of the beam. Comparing the experimental results of the shear force (V_{ex}) and the theoretical results (V_{th}) of the Egyptian code of practices (ECP-203)[18] was done. From the shear force diagram, it was found that the shear force is equal to the support reaction that is equal to half the vertical load. And the theoretical shear force is equal to the force for allowable concrete shear strength, as in Eq.(1) plus the force from carrying shear strength by vertical stirrups as in Eq(2).

Where f_{cu} is characteristic cube compressive strength of concrete in N/mm^2 , A_{st} is the area of stirrups, b is the section width, S is the spacing between stirrups. γ_c and γ_s are the material factor of safety of concrete and steel, respectively, and are taken as equal units in the calculation. Therefore, the theoretical shear force can be calculated as the following equation.

A comparison between the experimental shear force obtained from the test results and theoretical shear force prediction of the Egyptian Code are listed in Table 3. It can be seen that rational values are obtained in the case of $L/d=1.80$ than that of the case of $L/d = 2.0$. In general, the code equation is safe and more conservative in the case of $L/d = 1.80$ where the effect of size ratio on shear strength of the beam is obvious. For span-depth ratio of 1.80, adding glass fiber by 0.25%, 0.75% and 1.50% increased the shear force of the beam by 35%, 61% and 12%, than the predicted values of the code, respectively, while in case of span to depth ratio of 2.0, the increase in values is around 54%, 10%, for specimens B-5 and B-8 respectively. But For span-depth ratio of 2.20, adding glass fiber by 0.25%, 0.75% and 1.50% decreased the shear force of beam by 36% than the predicted values of the code. As the code does not take into consideration the effect of adding fibers. In addition, a comparison between the experimental results of the shear force (V_{ex}) and theoretical values (V_{th}) by ACI318 code is done. The theoretical shear force is equal to the force for concrete (V_c) taken factor load (ϕ) equal unity and the (V_s) force from stirrups. Therefore, the theoretical shear force can be calculated as the following equation.

Where f_c is cylinder compressive strength in psi, and taken 0.85 characteristic cube compressive strength (f_{cu}). A comparison between the experimental shear force obtained from test results and theoretical shear force prediction of ACI-318 are listed in Table 3. For span to depth ratio 1.80 by increasing fiber 0.25, 0.75 and 1.50% the ratio between experimental and theoretical increased 23%, 46%, respectively, and 5% for shear capacity, and for depth ratio 2.0, the ratio 0.25, 0.75 increased 34% and the ratio 1.50 decreased 8% for shear capacity. For the depth ratio 2.2, the results are different from previous results, where the shear capacity for beams decreased by 13%, 41% for mixed beams with GFRC. These results show that the codes (ECP and ACI 318) should be revised in the future as collected data with respect to the use of new adding materials.

Table 3: comparison between the experimental shear force obtained from test results and theoretical shear force prediction of ACI-318

Beam	Material	a/d	$\rho\%$	v_c (KN)	v_c (KN)	V_{ex}/V_{th}	V_c (KN)	V_{ex}/V_{th}
				Test	ECP-203		ACI-318	
S1	Control	1.8	0	110	86.73	1.27	100.75	1.09
S2	GFRC		0.25	125	87.48	1.35	101.51	1.23
S3	GFRC		0.75	150	88	1.61	102.61	1.46
S4	GFRC		1.5	105	86.13	1.12	99.98	1.05

S5	Control	2	0	125	86.73	1.44	100.75	1.24
S6	GFRC		0.25	135	87.48	1.54	101.51	1.34
S7	GFRC		0.75	135	88	1.53	102.61	1.34
S8	GFRC		1.5	95	86.13	1.1	99.98	0.92
S9	Control	2.2	0	100	86.73	1.15	100.75	0.99
S10	GFRC		0.25	90	87.48	1.03	101.51	0.87
S11	GFRC		0.75	60	88	0.68	102.61	0.59
S12	GFRC		1.5	55	86.13	0.64	99.98	0.54

Based on the strain compatibility and equilibrium conditions and suitable assumptions for HSFRC beam sections, the formulations of the proposed approach are presented. According to ACI Code (ACI Committee 318, 2005), the ultimate moment strength (M_u) is as follows:

$$M_u = (\text{strength reduction factor}) * M_n$$

Basic Assumptions of the Approach. The proposed approach for flexure of HSFRC beams is based on the following assumptions:

- Plane sections remain plane after bending, and consequently, the strain distribution is linear.
- The strain in the reinforcement is equal to the strain in concrete at the same level which implies a perfect bond between concrete and steel.
- For steel reinforcement in compression and tension, the bilinear elastoplastic idealization is used.
- For HSFRC in compression, the stress distribution is idealized by the equivalent rectangular stress block of ACI code (ACI Committee 318, 2005). A uniform stress of $0.67 f_{cu}$ is assumed to be distributed over an equivalent compression zone of depth = a , given as a function of the neutral axis depth c

$$a = \beta c$$

$$\beta = 1.05 - 0.05 (f_{cu} / 6.9) \quad 0.85 \geq \beta \geq 0.65$$

- Based on the study of plastic hinges, concrete is assumed to crush when the compression strain reaches a limiting usable strain which is taken as 0.003 (ACI Committee 544, 1988). It should be noted that the much higher limiting strains have been measured in HSFRC members.
- Using a perfectly plastic idealization for the behavior of HSFRC in tension, the tensile stress rectangular distribution is represented by a uniform stress which equals the post-cracking strength f_{pp} and acting over a depth of $(t - c)$. The post-cracking strength accounts for the pullout resistance of glass fibers.

Formulations of the Approach:

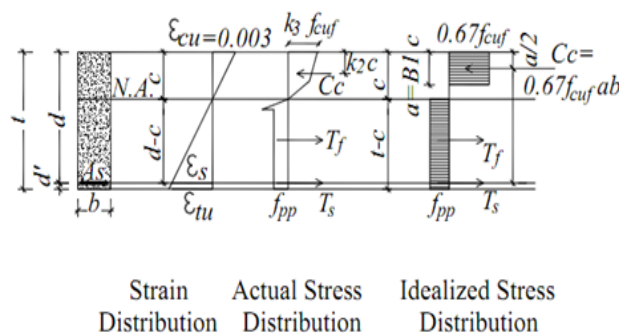


Figure (31): Fully Reinforced SFRC Section

Based on the above assumptions, the ultimate strain and stress distribution is shown in Fig.31 for the fully reinforced HSFRC section, where the glass fiber is included only in the tension side over a depth of t_f . From the force equilibrium condition and strain compatibility condition, the depth of the compression block can be determined as follows:

$$C_c = T_s + T_f$$

$$T_s = A_s f_s$$

$$\epsilon_s = 0.003(\beta d / a - 1)$$

$$f_s = E_s \epsilon_s < \epsilon_y$$

$$f_s = f_y \epsilon_s \geq \epsilon_y$$

For fully reinforced GFRC section, the forces C_c and T_f are given by:

$$C_c = 0.67 f_{cu} a b$$

$$T_f = 1.64 v_f (I_f / \Phi) b (t - c)$$

For the partially reinforced GFRC section, the forces are given by:

$$C_c = 0.67 f_{cu} a b$$

$$T_f = 1.64 v_f (I_f / \Phi) b t_f$$

From the equilibrium condition of moments, the nominal moment capacity of the fully reinforced GFRC section is expressed by:

$$M_n = T_s (d - \beta c / 2) + T_f [(t + c - \beta c) / 2]$$

Beam	Material	a/d	$\rho\%$	$M_{uex}(\text{KN.m})$	$M_n(\text{KN.m})$	M_{uex}/M_n
				Test	ACI	
S1	Control	1.8	0	44	30.78	1.43
S2	GFRC		0.25	50	32.2	1.55
S3	GFRC		0.75	60	34.83	1.72
S4	GFRC		1.5	42	31.02	1.35
S5	Control	2	0	56.2	30.78	1.83
S6	GFRC		0.25	60.75	32.2	1.89
S7	GFRC		0.75	60.75	34.83	1.74
S8	GFRC		1.5	42.75	31.02	1.38
S9	Control	2.2	0	50	30.78	1.62
S10	GFRC		0.25	45	32.2	1.39
S11	GFRC		0.75	27.5	34.83	0.79
S12	GFRC		1.5	30	31.02	0.96
Overall average						1.47
Overall standard deviation						0.48

There is a good agreement between the computed flexural strengths of the proposed ultimate strength state for GFRC beams, and the experimental results of several literature sources. Despite the difference in test specimens, concrete strength, reinforcement details, and fiber parameters. The predicted flexural strengths as computed by (ACI Committee 544, 1988) are very conservative where the mean value of the ratio between the measured and calculated strengths is 1.47 and the standard deviation is 0.48. The sensitivity studies of the governing fiber parameters indicate that the nominal moment capacity for a given GFRC section increases with the increase of fiber volume fraction and fiber aspect ratio. For different fiber contents, the predicted flexural strengths for partially reinforced GFRC beams are slightly less than that of fully reinforced SFRC beams. Also, the validation studies indicate the increase of nominal moment capacity with the increase of concrete strength, yield stress of steel, tension steel ratio, and compression steel ratio.

7. CONCLUSIONS

This study presents the results of an experimental study on the shear behavior of R.C. beams using glass fibers with different ratios. The following main conclusions can be drawn:

- 1) Using glass fibers increases the failure load, the efficiency of glass fibers helps reduce the crack width and make homogenous material advantage of ductility.
- 2) The failure mode becomes more ductile by using discrete glass fibers compared to the control beam specimens. On the other side, the number of the observed cracks increased and its widths decreased.

- 3) The used discrete glass fibers share both of longitudinal steel bars and of vertical stirrups as element resistance tensile strength after cracking.
- 4) For shearspan-depth ratio of 1.80, adding glass fiber by 0.25% and 0.75% increased the shear force of beam by 35% respectively, and 61%, than the predicted values of the ECP-203 code, respectively, while in case of the shear span to depth ratio of 2.0, the increase values were 10% and 54%, respectively.
- 5) The strut width of the compression zone of tested R.C. beams increases by increasing the percentages of the used glass fibers.
- 6) Modified ECP-203 code formulas are required for predicting the ultimate shear strength of high strength concrete mixed with discrete fiber.

There is a good agreement between the computed flexural strengths of the proposed ultimate strength state for HSFRC beams and the experimental results of several literature sources. Despite the difference in test specimens, concrete strength, reinforcement details, and fiber parameters, the proposed approach predicts the flexural strength reasonably well and proves its suitability as an analysis design tool. The mean value of the ratio between the measured and calculated strengths is 1.47 and the standard deviation is 0.48. The sensitivity studies of the governing fiber parameters indicate that the nominal moment capacity for a given HSFRC section increases with the increase of fiber volume fraction and fiber aspect ratio. For different fiber contents, the predicted flexural strengths for partially reinforced SFRC beams are slightly less than that of fully reinforced SFRC beams. Also, the validation studies indicate the increase of nominal moment capacity with the increase of concrete strength, yield stress of steel, tension steel ratio, and compression steel ratio.

REFERENCES

- [1] ACI Committee 544.4R (1988) (Reapproved 2002). "Design considerations for steel fiber reinforced concrete." ACI Structural Journal, 85(5), 563-580.
- [2] ACI Committee 318. Building code requirements for structural concrete (ACI 318) and commentary-ACI 318R-. American Concrete Institute; 2008.369 p.
- [3] Egyptian code of practice for design and construction of reinforced concrete structures; 2003.
- [4] Ata El-kareim S. Soliman. Efficiency of used glass fiber in concrete and reinforced concrete elements. PhD Thesis, Belgorod, Russia: Technology of Building Materials; 2005.
- [5] Altoubat S, Yazdanbankusn A, Rieder K. Shear behavior of macro-synthetic fiber-reinforced concrete without stirrups. ACI Mater J 2009;4(106):381-9.
- [6] Batson G, Jenkins E, Spatney R. Steel fibers as shear reinforcement in beams. ACI J 1972;10(69):640-4.
- [7] Bentz EC, Vecchio FJ, Collins MP. Simplified modified compression concrete elements. ACI Struct J 2006;4(103):614-24.
- [8] Al Sayed, S. H. (1993). "Flexural deflection of reinforced fibrous concrete beams." ACI Structural Journal, 90(1), 72-76.
- [9] Ashour, S. A., and Wafa, F. F. (1997), "Flexural behavior of high-strength fiber reinforced concrete beams." ACI Structural Journal, 90(3), 279-287.
- [10] Zararis PD, Zararis IP. Shear strength of reinforced concrete beams under uniformly distributed loads. ACI Struct J 2008;6(105):711-9.
- [11] Bayasi, Z., and Zeng, J., "Flexural Behavior of Slurry Infiltrated Mat Concrete (SIMCON)," Journal of Materials in Civil Engineering, V. 9, No. 4, Nov. 1997, pp. 194-199.
- [12] Naaman, A. E., and Reinhardt, H. W., "Proposed Classification of HPC Composites Based on Their Tensile Response," Materials and Structures, V.39, No. 289, June 2006, pp. 547-555.
- [13] Dupont, D., "Modelling and Experimental Validation of the Constitutive Law (σ - ϵ) and Cracking Behavior of Steel Fiber Reinforced Concrete" PhD dissertation, Catholic University of Leuven, Belgium, 2003